

A model for the structure of square-well fluids

S. Bravo Yuste^{a)}

Institute for Nonlinear Science and Department of Chemistry, University of California, San Diego, La Jolla, California 92093-0340

A. Santos

Departamento de Física, Universidad de Extremadura, E-06071 Badajoz, Spain

(Received 7 February 1994; accepted 18 April 1994)

A simple explicit expression for the Laplace transform of $rg(r)$ for 3D square-well fluids is proposed. The model is constructed by imposing the following three basic physical requirements: (a) $\lim_{r \rightarrow \sigma^+} g(r) = \text{finite}$, (b) $\lim_{q \rightarrow 0} S(q) = \text{finite}$, and (c) $\lim_{r \rightarrow \lambda \sigma^-} g(r) / \lim_{r \rightarrow \lambda \sigma^+} g(r) = \exp(\epsilon/k_B T)$. When applied to 1D square-well fluids, the model yields the exact radial distribution function. Furthermore, in the sticky-hard-sphere limit [$\lambda \rightarrow 1$, $\epsilon \rightarrow \infty$, $(\lambda - 1)\exp(\epsilon/k_B T) = \text{finite}$] the model reduces to Baxter's exact solution of the Percus–Yevick equation. Comparison with Monte Carlo simulation data shows that the model is a good extension of Baxter's solution to "thin" square-well fluids. For "wide" square-well fluids the model is still an acceptable approximation even for densities slightly above the critical density and temperatures slightly below the critical temperature.

I. INTRODUCTION

The study of square-well (SW) fluids is important as a means to understand the behavior of real fluids at and out of equilibrium. The SW interaction potential is

$$\varphi(r) = \begin{cases} \infty, & r < \sigma \\ -\epsilon, & \sigma < r < \lambda\sigma \\ 0, & r > \lambda\sigma, \end{cases} \quad (1.1)$$

where σ is the diameter of the hard core, ϵ is the well depth, and $(\lambda - 1)\sigma$ is the well width. The equilibrium properties of a SW fluid depend on the values of three dimensionless parameters: the reduced number density $\rho^* = \rho\sigma^3$, the reduced temperature $T^* = k_B T / \epsilon$ (k_B being the Boltzmann constant), and the width parameter λ . In the limits $\lambda \rightarrow 1$ and/or $\epsilon \rightarrow 0$ (i.e., $T^* \rightarrow \infty$), the SW fluid becomes the hard-sphere (HS) fluid. On the other hand, the sticky-hard-sphere (SHS) fluid¹ is obtained by taking the limits $\lambda \rightarrow 1$ and $\epsilon \rightarrow \infty$ (i.e., $T^* \rightarrow 0$) while keeping the parameter

$$\tau^{-1} = 12(1 - \lambda^{-1})e^{1/T^*} \quad (1.2)$$

constant. In the limit $\tau^{-1} \rightarrow 0$, the SHS fluid reduces to the HS fluid. Thus, at a given density ρ^* , the parameter space for SW fluids can be taken as the plane (τ^{-1}, λ) , it reduces to the line $(\tau^{-1}, \lambda = 1)$ for the SHS fluid and it shrinks to the point $(\tau^{-1}, \lambda) = (0, 1)$ for the HS fluid. This geometric picture shows that the generalizations from HS to SHS and from SHS to SW are not trivial at all.

Despite the mathematical simplicity of the SW potential, no analytical solution of the conventional integral equations for fluids (YBG, HNC, Percus–Yevick, ...) is known.² Therefore, information about the radial distribution function and the structure factor of SW fluids is usually obtained via Monte Carlo (MC) simulations, numerical solutions of inte-

gral equations, or perturbation theory.^{3–7} The mean spherical approximation of Sharma and Sharma⁸ provides an analytical expression for the structure factor, but it is not consistent with the hard core exclusion constraint.

The most popular integral equation is, perhaps, the Percus–Yevick (PY) equation.² It is exactly solvable for the HS interaction⁹ and, more generally, for the SHS interaction.¹ This is important, since the SHS fluid can be used to model the thermodynamical and structural properties of "thin" SW fluids (i.e., with $\lambda \leq 1.1$).^{10–12} Recently, these very short-ranged SW interactions have been used to explain the properties of systems such as colloidal particles, microemulsions, and micelles.^{7,12–14}

The aim of this paper is to propose a quasi-analytical model for the radial distribution function (RDF) $g(r)$ and, equivalently, the structure factor $S(q)$ of SW fluids. The model is constructed by assuming for a function $F(r)$ related to the Laplace transform of $rg(r)$ a form suggested by its exact low-density behavior and consistent with the following physical requirements: (a) $g(r)$ is finite at $r = \sigma$, (b) $S(q)$ is finite at $q = 0$ or, equivalently, the isothermal compressibility is finite, and (c) $y(r) \equiv e^{\varphi(r)/k_B T} g(r)$ is continuous at $r = \lambda\sigma$. We have recently shown^{15–17} that the same method as applied to the HS and SHS cases yields the respective exact solutions of the PY equation. Therefore, our model can be seen as a generalization to SW fluids of the analytical expressions obtained from the PY equation for HS and SHS fluids. Consequently, the model is especially useful for short-ranged SW fluids, its quality worsening as λ increases.

This paper is organized as follows. Basic definitions and useful equations are presented in Sec. II. The model is introduced and worked out in Sec. III. Section IV deals with the comparison with MC simulation results. The paper ends with a brief discussion in Sec. V.

II. BASIC DEFINITIONS

The RDF $g(r)$ of a fluid is directly related to the probability of finding two particles separated by a distance r .²

^{a)}Permanent address: Departamento de Física, Universidad de Extremadura, E-06071 Badajoz, Spain.

Thus, it contains information about the spatial structure as well as the thermodynamic properties of the fluid. In real fluids the RDF can be determined from neutron or x-ray diffraction experiments, which measure the static structure factor $S(q)$. Both quantities are related by Fourier transforms:

$$S(q) = 1 + \rho \int dr e^{-iq \cdot r} h(r), \quad (2.1)$$

where $h(r) \equiv g(r) - 1$ is the net correlation function and ρ is the number density. A formal representation of $g(r)$ is given by means of a power series expansion:

$$y(r) \equiv e^{\varphi(r)/k_B T} g(r) = 1 + \sum_{n=1}^{\infty} y_n(r) \rho^n. \quad (2.2)$$

From a practical point of view, however, this representation is only useful at low densities. The exact expression of $y_1(r)$ for SW fluids is given, for instance, in Ref. 18.

Henceforth we will restrict ourselves to three-dimensional fluids with a hard core at $r = \sigma$. Let us now introduce the Laplace transform $G(t)$ of $rg(r)$:

$$G(t) = \int_1^{\infty} dr e^{-rt} rg(r), \quad (2.3)$$

where we have taken the hard-core diameter σ as length unit. We take the Laplace transform of $rg(r)$, rather than that of $g(r)$, in order to relate it in a simple way to the Fourier transform of $g(r)$. Thus, the structure factor can be obtained from $G(t)$ as

$$S(q) = 1 - 24 \eta \text{Re} \lim_{t \rightarrow iq} t^{-1} [G(t) - t^{-2}], \quad (2.4)$$

where $\eta \equiv (\pi/6) \rho^*$. The isothermal compressibility is directly connected to $S(0)$. In previous works,¹⁵⁻¹⁷ we have found it convenient to define an auxiliary function $F(t)$ through the relation

$$G(t) = t \frac{F(t)e^{-t}}{1 + 12 \eta F(t)e^{-t}} = \sum_{n=1}^{\infty} (-12 \eta)^{n-1} t [F(t)]^n e^{-nt}. \quad (2.5)$$

Laplace inversion of Eq. (2.5) provides a useful representation of the RDF:

$$g(r) = r^{-1} \sum_{n=1}^{\infty} (-12 \eta)^{n-1} f_n(r-n) \Theta(r-n), \quad (2.6)$$

where $f_n(r)$ is the inverse Laplace transform of $t[F(t)]^n$ and $\Theta(r)$ is Heaviside's step function. Only the n first terms in the summation are needed to determine $g(r)$ for $r < n + 1$. The series (2.2) and (2.6) are quite different; while the coefficients $y_n(r)$ in Eq. (2.2) are density-independent, the coefficients $f_n(r)$ in Eq. (2.6) do depend on density.

Thus, the knowledge of $F(t)$ is fully equivalent to that of $g(r)$ or $S(q)$. In particular, the value of $g(r)$ at contact point, $g(1^+)$, is given by the asymptotic behavior of $F(t)$ for large t :

$$g(1^+) = f_1(0) = \lim_{t \rightarrow \infty} t^2 F(t). \quad (2.7)$$

On the other hand, according to Eq. (2.4), the behavior of $G(t)$ for small t determines the value of $S(0)$:

$$G(t) = t^{-2} + \text{const} + \frac{1 - S(0)}{24 \eta} t + o(t^2). \quad (2.8)$$

On physical grounds, both $g(1^+)$ and $S(0)$ must be finite in a disordered fluid. The first condition yields, on account of Eq. (2.7),

$$F(t) \sim t^{-2}, \quad t \rightarrow \infty. \quad (2.9)$$

By inserting Eq. (2.8) into the first equality of Eq. (2.5), the condition $S(0) = \text{finite}$ fixes the first five terms in the expansion of $F(t)$ in powers of t :¹⁵

$$F(t) = -\frac{1}{12 \eta} \left(1 + t + \frac{1}{2} t^2 + \frac{1 + 2 \eta}{12 \eta} t^3 + \frac{2 + \eta}{24 \eta} t^4 \right) + \mathcal{O}(t^5). \quad (2.10)$$

It is remarkable how these two rather weak conditions restrict so much the behavior of $F(t)$ for large and small t . Nevertheless, there are still an infinite number of forms for $F(t)$ compatible with Eqs. (2.9) and (2.10). In fact, both equations are so general that they do not include the temperature and apply to any hard-core potential. In order to gain insight into the features of $F(t)$ which are characteristic of a given potential, it is useful to consider its exact form up to first order in density. In the case of a SW fluid with $\lambda < 2$, one can get from Ref. 18 the following structure for $F(t)$:

$$F(t) = R(t) - \bar{R}(t) e^{-(\lambda-1)t}, \quad (2.11)$$

where

$$R(t) = t^{-3} (1+x)(1+t) + t^{-6} \{ 12(1+x)(1+t) + 6[2x^2(\lambda^2-1) + x(2\lambda^2-3) - 1]t^2 - 2[2x^2(\lambda-1)^2(2\lambda+1) + x(4\lambda^3-6\lambda^2+3) + 1]t^3 + [3x^3(\lambda^2-1)^2 + 2x^2(\lambda-1)(3\lambda^3-\lambda^2-4\lambda-4) + x(3\lambda^4-8\lambda^3+\frac{15}{2}) + \frac{5}{2}]t^4 \} \eta + \mathcal{O}(\eta^2), \quad (2.12)$$

$$\bar{R}(t) = t^{-3} x(1+\lambda t) + t^{-6} x \{ 12(1+\lambda t) + 6[2x(\lambda^2-1) + \lambda^2 - 2]t^2 + 2[2x(\lambda-1)^2(\lambda+2) + (\lambda-2)(\lambda^2+2\lambda-2)]t^3 + [3x^2(\lambda^2-1)^2 + x(\lambda-3)(\lambda-1)(\lambda^2+4\lambda+1) + \frac{1}{2}\lambda(\lambda-2)^2(\lambda+4)]t^4 \} \eta + \mathcal{O}(\eta^2). \quad (2.13)$$

In these equations, $x \equiv e^{1/T^*} - 1$. Equations (2.10)–(2.13) show that $F(t)$ is singular in the double limit $t \rightarrow 0$, $\eta \rightarrow 0$.

III. THE MODEL

All the equations of the previous sections are exact. Our objective now is to propose a simple functional form for $F(t)$ consistent with the behaviors (2.9) and (2.10). In the HS and SHS cases,¹⁵⁻¹⁷ we proposed rational-function forms, i.e., Padé approximants, for $F(t)$. The approximations containing the least number of parameters turned out to co-

incide with the corresponding solutions of the PY equation. Following the same line of reasoning and taking into account the exact low density behavior, Eqs. (2.11)–(2.13), we propose rational forms for $R(t)$ and $\bar{R}(t)$ in Eq. (2.11). More specifically,

$$R(t) = -\frac{1}{12\eta} \frac{A^{(0)} + A^{(1)}t}{1 + S^{(1)}t + S^{(2)}t^2 + S^{(3)}t^3}, \quad (3.1)$$

$$\bar{R}(t) = -\frac{1}{12\eta} \frac{\bar{A}^{(0)} + \bar{A}^{(1)}t}{1 + S^{(1)}t + S^{(2)}t^2 + S^{(3)}t^3}. \quad (3.2)$$

$$F(t) = -\frac{1}{12\eta} \frac{1 + L^{(1)}t + L^{(2)}t^2 - [\bar{A}^{(0)} + L^{(2)}(\lambda - 1)^{-1}t][e^{-(\lambda-1)t} - 1 + (\lambda - 1)t]}{1 + S^{(1)}t + S^{(2)}t^2 + S^{(3)}t^3}, \quad (3.3)$$

where we have taken into account that

$$A^{(0)} = 1 + \bar{A}^{(0)}, \quad (3.4)$$

since $F(0) = -1/12\eta$, and we have called

$$L^{(2)} \equiv \bar{A}^{(1)}(\lambda - 1), \quad (3.5)$$

$$L^{(1)} \equiv \bar{A}^{(0)}(\lambda - 1) + A^{(1)} - \bar{A}^{(1)}. \quad (3.6)$$

These changes have been introduced to emphasize the interpretation of Eq. (3.3) as a generalization to the SW interaction of the analytic solution of the PY equation for the SHS interaction. In that case, the expression for $F(t)$ is¹⁶

$$F(t) = -\frac{1}{12\eta} \frac{1 + L^{(1)}t + L^{(2)}t^2}{1 + S^{(1)}t + S^{(2)}t^2 + S^{(3)}t^3}. \quad (3.7)$$

The model (3.3) contains six parameters to be determined. The exact expansion (2.10) imposes four constraints among them. Thus, we can express four of the parameters in terms of, for instance, $\bar{A}^{(0)}$ and $L^{(2)}$. The result is

$$L^{(1)} = \frac{1}{1 + 2\eta} \left[1 + \frac{1}{2}\eta + 6\eta\lambda L^{(2)} - \eta(\lambda - 1)^2(3\bar{A}^{(0)} - 2L^{(2)}) - \frac{1}{2}\eta(\lambda + 3)(\lambda - 1)^3\bar{A}^{(0)} \right], \quad (3.8)$$

$$S^{(1)} = \frac{\eta}{1 + 2\eta} \left[-\frac{3}{2} + 6\eta L^{(2)} - (\lambda - 1)^2(3\bar{A}^{(0)} - 2L^{(2)}) - \frac{1}{2}(\lambda + 3)(\lambda - 1)^3\bar{A}^{(0)} \right], \quad (3.9)$$

$$S^{(2)} = \frac{1}{2(1 + 2\eta)} \left\{ -1 + \eta + 2[1 - 2\eta(3\lambda - 1)]L^{(2)} - (\lambda - 1)^2[\bar{A}^{(0)} + 4\eta(L^{(2)} - \bar{A}^{(0)})] + \eta(\lambda + 3)(\lambda - 1)^3\bar{A}^{(0)} \right\}, \quad (3.10)$$

$$S^{(3)} = \frac{1}{1 + 2\eta} \left\{ -\frac{(1 - \eta)^2}{12\eta} - \left[\frac{1}{2}(\lambda + 1) - \eta(2\lambda - 1) \right] L^{(2)} + \frac{1}{2}(\lambda - 1)^2[\bar{A}^{(0)} + \eta(2L^{(2)} - \bar{A}^{(0)})] + \frac{1}{12}[2 - \eta(3\lambda + 5)](\lambda - 1)^3\bar{A}^{(0)} \right\}. \quad (3.11)$$

Equation (3.1) is sufficient to satisfy the requirement (2.9), so that Eq. (2.9) does not impose any constraint on $\bar{R}(t)$. We have taken for $\bar{R}(t)$ a form similar to that of $R(t)$ because, according to Eqs. (2.12) and (2.13), both functions have a similar structure in the low-density limit. In addition, we have chosen a common denominator in order to recover the SHS form for $F(t)$ in the limits $\lambda \rightarrow 1$, $x \rightarrow \infty$, $x(\lambda - 1) = \text{fixed}$.¹⁶

Thus, the function $F(t)$ is given in our model as

We need two additional constraints to determine the six parameters. One of those constraints is given by the (exact) continuity condition of the function $y(r)$ at $r = \lambda$.² This implies

$$g(\lambda^-) = (1 + x)g(\lambda^+). \quad (3.12)$$

Let us implement this condition on our model, Eq. (3.3). We denote by $\xi(r)$ and $\bar{\xi}(r)$ the inverse Laplace transforms of $tR(t)$ and $t\bar{R}(t)$, respectively. Then, if $\lambda < 2$, Eq. (2.6) gives

$$g(r) = r^{-1}[\xi(r - 1) - \bar{\xi}(r - \lambda)\Theta(r - \lambda)], \quad 1 < r < 2. \quad (3.13)$$

Condition (3.12) yields

$$(1 + x)\bar{\xi}(0) = x\xi(\lambda - 1). \quad (3.14)$$

Now, according to our model,

$$\xi(r) = -\frac{1}{12\eta} \sum_{i=1}^3 \frac{A^{(0)} + A^{(1)}z_i}{z_i[S^{(1)} + 2S^{(2)}z_i + 3S^{(3)}z_i^2]} e^{rz_i}, \quad (3.15)$$

where z_1 , z_2 , and z_3 are the roots of the denominator in Eqs. (3.1)–(3.3). Consequently, Eq. (3.14) becomes

$$(1 + x)\frac{\bar{A}^{(1)}}{S^{(3)}} = x \sum_{i=1}^3 \frac{A^{(0)} + A^{(1)}z_i}{z_i[S^{(1)} + 2S^{(2)}z_i + 3S^{(3)}z_i^2]} e^{(\lambda-1)z_i}, \quad (3.16)$$

where we have taken into account that

$$\bar{\xi}(0) = \lim_{t \rightarrow \infty} t^2 \bar{R}(t) = -\frac{1}{12\eta} \frac{\bar{A}^{(1)}}{S^{(3)}}. \quad (3.17)$$

Equation (3.16) is a transcendent equation. Given a value of $\bar{A}^{(0)}$, the set of Eqs. (3.8)–(3.11) and (3.16) can be solved to yield $L^{(1)}$, $L^{(2)}$, $S^{(1)}$, $S^{(2)}$, and $S^{(3)}$. All we have done is to propose the model (3.3) and then impose the basic exact conditions (2.10) and (3.12).

It still remains to determine the parameter $\bar{A}^{(0)}$. Since we are not aware of any additional basic condition valid at any density, we resort to the obvious condition $\lim_{\eta \rightarrow 0} y(r) = 1$. Let us call $\bar{A}_0^{(0)} \equiv \lim_{\eta \rightarrow 0} \bar{A}^{(0)}$, $L_0^{(2)} \equiv \lim_{\eta \rightarrow 0} L^{(2)}$. Then, the zero-density limit of Eq. (3.3) is

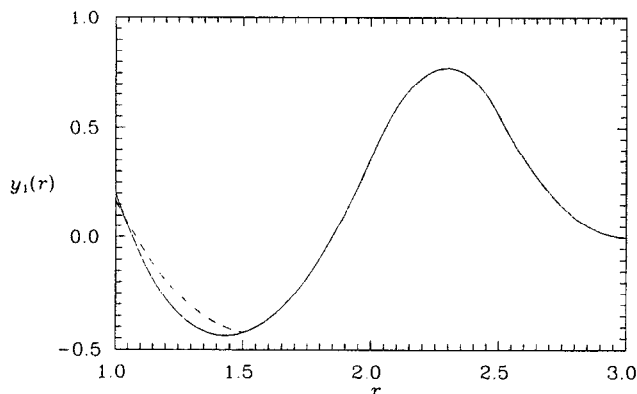


FIG. 1. Plot of the first order coefficient, $y_1(r)$, in the density expansion of $y(r)$ for $x=1$ and $\lambda=1.5$. The solid line is the exact result, while the dashed line is the result obtained from the model.

$$\lim_{\eta \rightarrow 0} F(t) = t^{-3} \{ 1 + \bar{A}_0^{(0)} + [1 - \bar{A}_0^{(0)}(\lambda - 1) + L_0^{(2)}(\lambda - 1)^{-1}] t - [\bar{A}_0^{(0)} + L_0^{(2)}(\lambda - 1)^{-1}] t^2 e^{-(\lambda-1)t} \}. \quad (3.18)$$

Condition (3.12) yields $L_0^{(2)} = x\lambda(\lambda - 1)$. Finally, Eq. (3.18) becomes exact if and only if $\bar{A}_0^{(0)} = x$.

The evaluation of the model up to first order in density is carried out in Appendix A. It is proved there that the difference $\Delta y_1(r)$ between the approximate and the exact first order coefficient in the density expansion (2.2) is

$$\Delta y_1(r) \Theta(r-1) = \frac{\pi}{6} \frac{r-\lambda}{r} \left\{ \frac{\bar{A}_1^{(0)}}{1+x} + x(\lambda-1)[(\lambda-1)^2 - 3(\lambda+1)(r-1)] \right\} [\Theta(r-1) - \Theta(r-\lambda)], \quad (3.19)$$

where $\bar{A}_1^{(0)}$ is defined as the linear coefficient of the density expansion of $\bar{A}^{(0)}$ [see Eq. (A5)]. We see that our model leads to an inexact function $y_1(r)$ in the interval $1 < r < \lambda$. This discrepancy is not important in the case of thin SW potentials and disappears in the SHS and HS limits. There does not seem to be an obvious criterion to choose $\bar{A}_1^{(0)}$. The criterion $\Delta y_1(1) = 0$ leads to $\bar{A}_1^{(0)} = -x(1+x)(\lambda-1)^3$, while the criterion of least mean square deviation leads to a positive choice of $\bar{A}_1^{(0)}$. As a compromise guided by simplicity, we choose $\bar{A}_1^{(0)} = 0$. Figure 1 shows the exact and the approximate functions $y_1(r)$ in the case $\lambda=1.5$, $x=1$ for this value of $\bar{A}_1^{(0)}$.

This analysis of the low density behavior of the model does not suffice to determine the parameter $\bar{A}^{(0)}$ at an arbitrary density η . For the sake of simplicity, however, we will identify $\bar{A}^{(0)}$ with its exact zero-density value, i.e.,

$$\bar{A}^{(0)} = x. \quad (3.20)$$

Then, the remaining five coefficients of the model are obtained from Eqs. (3.8)–(3.11) and (3.16). Once these coeffi-

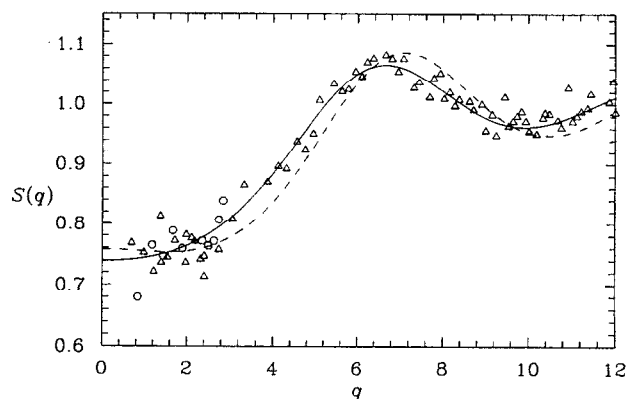


FIG. 2. Structure factor, $S(q)$, corresponding to a SW fluid with $\lambda=1.1$, $\eta=0.07$, and $T^{*-1}=0.92$. The circles and triangles are MC data taken from Fig. 3 of Ref. 7. The solid line is the result predicted by the model and the dashed line is the result obtained from the solution of the PY equation for SHS.

icients are known at given values of η , T^* , and λ , Eq. (3.3) provides the explicit expression of the function $F(t)$ in our model and, hence, the explicit expressions of $g(r)$ and $S(q)$. Appendix B shows that in the limit $x \rightarrow \infty$, $\lambda \rightarrow 1$, $x(\lambda - 1) = 1/12 \tau = \text{const}$, we recover the results obtained in Ref. 16 for the SHS potential. In that case, our model coincides with the analytical solution of the PY equation. On this basis, one can expect our model to be a fair approximation in the case of *thin* SW potentials.

The same line of reasoning followed here can be easily applied to the one-dimensional SW fluid. This is done in Appendix C. It is shown there that the model coincides with the *exact* solution to the problem, which can be obtained from the work of Salsburg, Zwanzig, and Kirkwood.¹⁹ This fact gives extra support to our model, Eq. (3.3), as a useful simple approximation.

IV. COMPARISON WITH MONTE CARLO SIMULATIONS

According to the previous section, we expect our model to be especially adequate to describe the structural properties of thin SW fluids. In 1984, Huang *et al.*⁷ performed MC simulations of SW fluids with $\lambda=1.02$ and $\lambda=1.1$ to reproduce the main features of the structure factor of microemulsions and micelles, respectively. Recently, Menon *et al.*¹¹ have compared the simulation data from Ref. 7 with the PY analytical solution for SHS with appropriate values of τ and η . Figure 2 shows $S(q)$ obtained from simulation⁷ for $\lambda=1.1$, $T^{*-1}=0.92$, and $\eta=0.07$ as compared with the PY solution for SHS (dashed line) and with our model (solid line). The results show that our model correctly accounts for changes in $S(q)$ associated to the non-zero width ($\lambda \neq 1$) of the square well. In fact, our results are practically indistinguishable from those obtained by numerical solution of the PY and MHNC equations,¹² the agreement with simulation in the small- q region being better than that observed in Ref. 7 with a mean spherical approximation. In the case of micro-

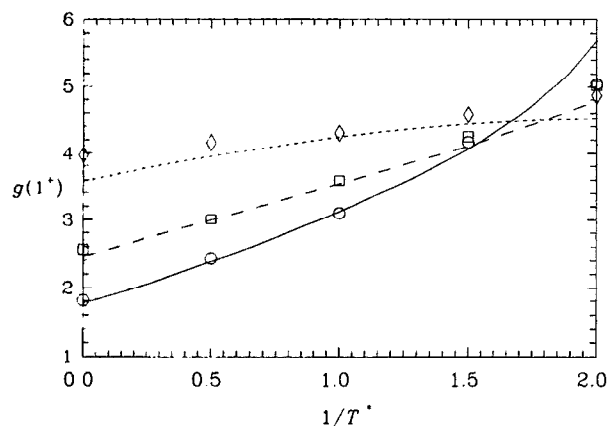


FIG. 3. Plot of $g(1^+)$ as a function of $1/T^*$ for $\lambda=1.125$ and three densities: $\rho^*=0.4$ (O and —), $\rho^*=0.6$ (□ and - - -), and $\rho^*=0.8$ (◇ and - · - ·). The symbols represent MC data taken from Ref. 5 ($1/T^* \neq 0$) and from Ref. 3 ($1/T^*=0$). The lines are the results given by the model.

emulsions ($\lambda=1.02$), the structure factor predicted by our model is hardly distinguishable from that given by the PY solution for SHS and both approximations agree well with simulation.

Henderson and co-workers^{5,6} have carried out rather extensive MC simulations of SW fluids for several values of λ . Figures 3 and 4 show the values of $g(r)$ at $r=1^+$ and $r=\lambda^-$, respectively, as functions of $1/T^*$ for $\lambda=1.125$ and $\rho^*=0.4, 0.6$, and 0.8 . The points at $1/T^*=0$ correspond to HS, in which case our model coincides with Wertheim–Thiele’s solution of the PY equation and underestimates $g(1^+)$ at high densities. As the temperature decreases, both theory and simulation indicate that $g(1^+)$ and $g(\lambda^-)$ tend to increase. The quantitative agreement worsens at low temperatures ($1/T^*=2$), although the theory succeeds in showing up that $g(1^+)$ and $g(\lambda^-)$ are greater for $\rho^*=0.4$ than for $\rho^*=0.8$ in the low temperature region.

Figures 5 and 6 are similar to Figs. 3 and 4, but for a wider well ($\lambda=1.25$). As expected, the agreement is worse now, especially at high densities and/or low temperatures.

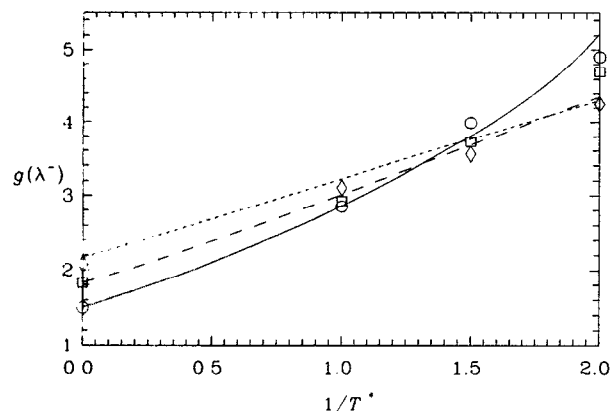


FIG. 4. The same as in Fig. 3, but for $g(\lambda^-)$.

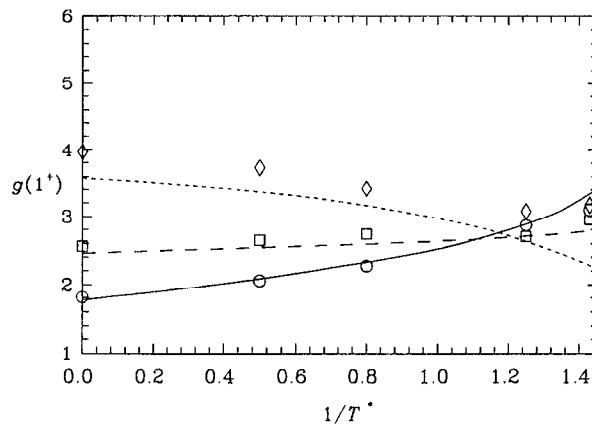


FIG. 5. The same as in Fig. 3, except that $\lambda=1.25$.

Despite this, our model correctly predicts that $g(1^+)$ at $\rho^*=0.8$, in contrast to what happens with $\lambda=1.125$, tend to decrease as the temperature decreases.

In order to assess the degree of reliability of our model when one goes from the HS fluid to a wide SW fluid at a given temperature, Fig. 7 shows $g(1^+)$ versus λ at $T^*=2$ and $\rho^*=0.4, 0.6$, and 0.8 .²⁰ At the density $\rho^*=0.4$ the agreement is excellent, even for $\lambda=1.85$, in which case $T^*=2$ is a subcritical temperature.⁵ At $\rho^*=0.6$ and 0.8 the agreement is reasonably good for $\lambda \leq 1.5$ and $\lambda \leq 1.25$, respectively. For wider wells, the theoretical values of $g(1^+)$ rapidly fall down and eventually the set of Eqs. (3.8)–(3.11) and (3.16) ceases to have a solution.

In Figs. 3–7 we have used the points $r=1$ and $r=\lambda$ to monitor the agreement between our model and simulation data. Now we are going to compare the respective radial distribution functions $g(r)$ for some representative cases. From Figs. 3 and 4 we concluded that a good agreement can be expected if $\lambda=1.125$, even for relatively large densities and low temperatures. This is confirmed by Fig. 8, where the case $\rho^*=0.8$, $T^*=1$ is considered. The agreement in the region $r > \lambda$ is better than in the region $1 < r < \lambda$. This might

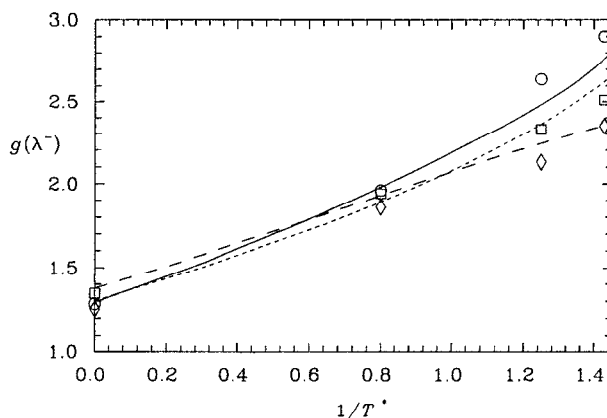


FIG. 6. The same as in Fig. 4, except that $\lambda=1.25$.

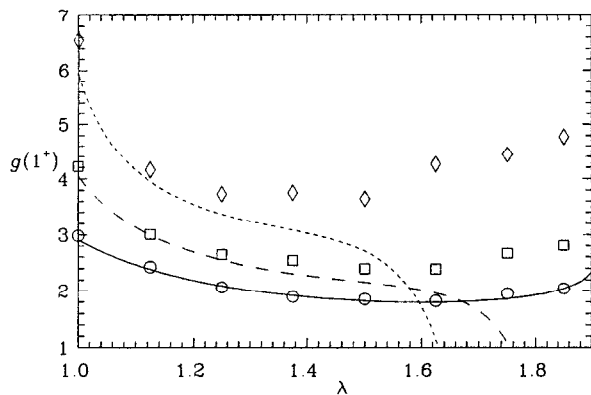


FIG. 7. Plot of $g(1^+)$ as a function of λ for $T^*=2$ and three densities: $\rho^*=0.4$ (\circ and $-$), $\rho^*=0.6$ (\square and $- -$), and $\rho^*=0.8$ (\diamond and $- -$). The symbols represent MC data taken from Ref. 5 ($\lambda \neq 1$) and from Ref. 3 ($\lambda = 1$; see Ref. 20). The lines are the results given by the model.

be a remnant of the fact that our model is not exact to first order in density in the latter region.

Let us now consider the well width $\lambda = 1.5$, which is usually taken as adequate to model the molecular interactions in argon. Figure 9 compares $g(r)$ obtained from simulation and from our model for the state $\rho^*=0.5$, $T^*=1$. The agreement is surprisingly good, especially if one considers that in this state the fluid is in the liquid phase and that our model, by construction, is expected to yield an accurate representation of the structural properties of *thin* SW fluids only. On the other hand, as the density increases, the reliability of the model decreases. We already saw in Fig. 7 that at $T^*=2$ and $\rho^*=0.8$ the value of $g(1^+)$ is clearly underestimated in the case $\lambda = 1.5$. Figure 10 shows that the overall prediction for $g(r)$ is not as poor as one might anticipate. The jump at $r = \lambda$ is described fairly well, as well as the behavior in the region $r > \lambda$.

It must be emphasized that the set of equations satisfied by the parameters of the model fail to have a solution for densities sufficiently high, temperatures sufficiently low, and

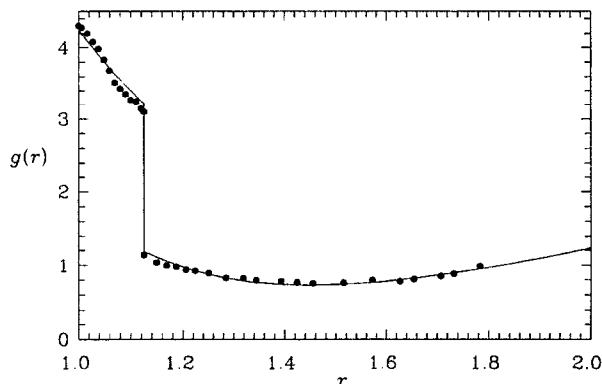


FIG. 8. Plot of the radial distribution function for $\lambda = 1.125$, $T^*=1$, and $\rho^*=0.8$. The dots represent MC data taken from Ref. 6, which were plotted in Fig. 1 of Ref. 5. The line is the result given by the model.

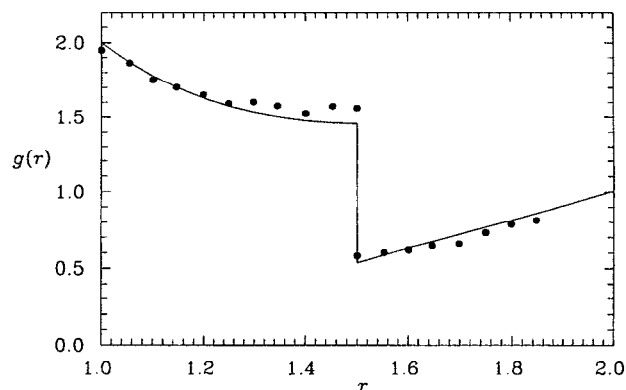


FIG. 9. Plot of the radial distribution function for $\lambda = 1.5$, $T^*=1$, and $\rho^*=0.5$. The dots represent MC data taken from Ref. 4. The line is the result given by the model.

wells sufficiently wide. This is the case, for instance, if $\rho^*=0.8$, $T^* = \frac{2}{3}$, and $\lambda = 1.5$. We have observed that this lack of a solution is mainly due to our choice for the parameter $\bar{A}^{(0)}$ of its exact zero-density value, Eq. (3.20). If, instead, we adjust the value of $\bar{A}^{(0)}$ as to fit the simulation value of $g(1^+)$, then we get a solution. The result obtained in this way for $\rho^*=0.8$, $T^* = \frac{2}{3}$, and $\lambda = 1.5$ is compared with MC simulation data in Fig. 11. As expected, the agreement near the contact point is good, but deviations are quite apparent when approaching $r = \lambda$ from the left. The details of $g(r)$ in the region $r > \lambda$ are not well described either. The dashed curve in Fig. 10 represents the result obtained under the same criterion in the case $\rho^*=0.8$, $T^*=2$, and $\lambda = 1.5$. Since the temperature now is higher than before, the agreement is much better. On the other hand, this modification of our model implies to empirically fit the parameter $\bar{A}^{(0)}$. It would be preferable to find an independent simple criterion to determine $\bar{A}^{(0)}$ as a function of ρ^* , T^* , and λ . Of course,

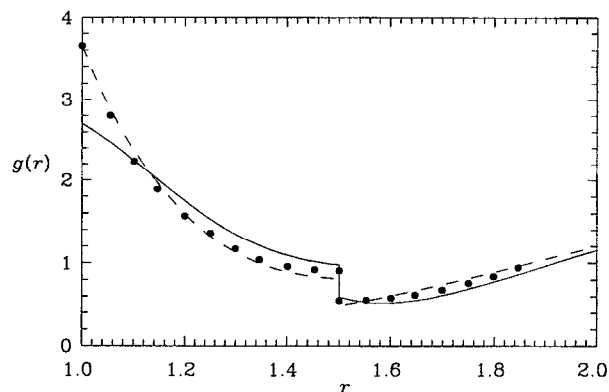


FIG. 10. Plot of the radial distribution function for $\lambda = 1.5$, $T^*=2$, and $\rho^*=0.8$. The dots represent MC data taken from Ref. 4. The solid line is the result given by the model ($\bar{A}^{(0)} = x$), while the dashed line corresponds to a modification of the model in which the value of the parameter $\bar{A}^{(0)}$ is adjusted to fit the simulation value of $g(1^+)$.

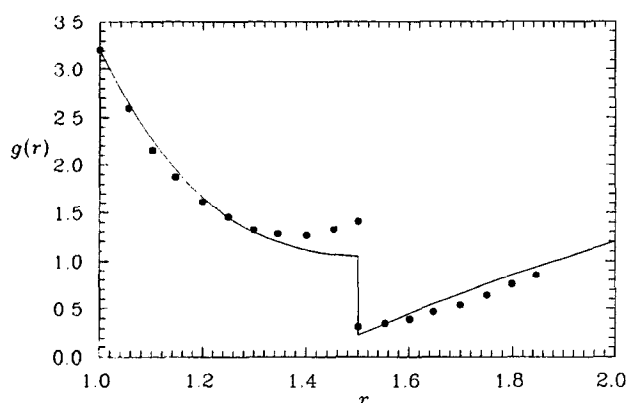


FIG. 11. Plot of the radial distribution function for $\lambda=1.5$, $T^*=\frac{2}{3}$, and $\rho^*=0.8$. The dots represent MC data taken from Ref. 4. The line corresponds to a modification of the model in which the value of the parameter $\bar{A}^{(0)}$ is adjusted to fit the simulation value of $g(1^+)$.

such a criterion should reduce in the zero-density limit to the one adopted along this paper, Eq. (3.20).

V. SUMMARY AND DISCUSSION

In this paper we have proposed a very simple model for the structure of a square-well (SW) fluid of (relative) width $\lambda - 1 < 1$. The model consists of assuming rational forms for the functions $R(t)$ and $\bar{R}(t)$ defined in Eq. (2.11), where $F(t)$ is a function related by Eq. (2.5) to the Laplace transform $G(t)$ of $rg(r)$. The knowledge of $F(t)$ allows one to get an analytical expression for the radial distribution function (RDF) $g(r)$, Eq. (2.6), as well as for the structure factor $S(q)$, Eq. (2.4). We impose on our model the following three basic conditions: (a) $g(1^+) = \text{finite}$; (b) $S(0) = \text{finite}$; (c) $g(\lambda^-)/g(\lambda^+) = \exp(1/T^*)$. By construction, the rational-function forms for $R(t)$ and $\bar{R}(t)$, Eqs. (3.1) and (3.2), are consistent with condition (a). Then, condition (b) establishes five (algebraic) constraints among the seven parameters characterizing $R(t)$ and $\bar{R}(t)$. Condition (c) yields a sixth (transcendent) constraint. In order to determine all the parameters, one of them must be fixed. We have chosen to assign to $\bar{A}^{(0)}$ its exact zero-density value, which turns out to be independent of λ . This closes the construction of our model.

Although conditions (a)–(c) are apparently rather vague and general, their implementation on the model gives rise to a non-trivial approximation. This is supported by two facts: (i) the same arguments translated to the one-dimensional case yields the *exact* solution to the problem; (ii) in the special limit of sticky hard spheres [$\lambda \rightarrow 1$, $T^* \rightarrow 0$, $(\lambda - 1)\exp(1/T^*) = \text{finite}$] our model reduces to Baxter's exact solution of the PY equation. As a consequence of the latter, (iii) our model reduces to Wertheim-Thiele's exact solution of the PY equation in the particular case of hard spheres ($\lambda = 1$ or $T^* \rightarrow \infty$).

Due to the simplicity of the model, the RDF to first order in density is not exact in the interval $1 < r < \lambda$. This is not a serious drawback, since the density expansion of the RDF fails to converge even at temperatures and volumes significantly greater than the critical temperature and volume.¹⁸

Furthermore, on the basis of the fact (ii), our model is expected to be a good approximation in the case of *thin* SW fluids (say $\lambda \leq 1.1$). Thin SW fluids are very useful tools to analyze properties of colloids, micelles, microemulsions, and other systems exhibiting percolation behavior.^{7,12–14,21} Baxter's solution of the PY equation for SHS has been usually considered as an adequate model for such systems.^{10–12,22} On the other hand, our model allows one to "correct" Baxter's solution by incorporating effects associated to a non-zero attractive-well width.

It must be stressed that the model is not constructed as a perturbation correction to the PY solution for SHS fluids. Consequently, it can be applied in principle to *wide* SW fluids. The comparison with Monte Carlo results shows a much better agreement than one could expect. At high densities ($\rho^* = 0.8$, for instance) it is well-known that the PY approximation is not good enough in the case of hard spheres. Thus, it is not surprising that the model fails (and eventually has no solution) as the temperature decreases and/or the well width increases. However, at moderate densities (say $\rho^* = 0.4$, which is greater than the typical critical density), the agreement is pretty good even for temperatures below, but near, the critical temperature.

The model proposed in this paper is not fully analytical, since one of the equations satisfied by the parameters is transcendental. This is not surprising, as the exact solution of the one-dimensional problem also involves a similar transcendental equation. Nevertheless, the numerical evaluation of the parameters can be easily carried out.²³ On the other hand, if the model is applied to thin SW fluids, Eq. (3.12) can be expanded in powers of $\lambda - 1$ to yield an algebraic, rather than a transcendental, equation. Work is now in progress along this line.

ACKNOWLEDGMENTS

We are very grateful to Professor D. Henderson for providing us with the Monte Carlo data of Fig. 8. Partial support from the Dirección General de Investigación Científica y Técnica (MEC, Spain) through Grant No. PB91-0316 is gratefully acknowledged.

APPENDIX A: LOW-DENSITY BEHAVIOR OF THE MODEL

In the low-density limit, Eqs. (3.8)–(3.11) become, respectively,

$$L^{(1)} = 1 - \frac{3}{2}\eta[1 - x(\lambda^4 - 1)] + \mathcal{O}(\eta^2), \quad (\text{A1})$$

$$S^{(1)} = \mathcal{O}(\eta), \quad (\text{A2})$$

$$S^{(2)} = -\frac{1}{2}[1 - x(\lambda^2 - 1)] + \mathcal{O}(\eta), \quad (\text{A3})$$

$$S^{(3)} = -\frac{1}{12\eta} + \frac{1}{3}[1 - x(\lambda - 1)(\lambda^2 + \lambda + 1)] + \mathcal{O}(\eta). \quad (\text{A4})$$

The other two parameters are

$$\bar{A}^{(0)} = x + \bar{A}_1^{(0)}\eta + \mathcal{O}(\eta^2), \quad (\text{A5})$$

$$L^{(2)} = x\lambda(\lambda - 1) + L_1^{(2)}\eta + \mathcal{O}(\eta^2). \quad (\text{A6})$$

Substitution into Eq. (3.3) yields, after some algebra,

$$F(t) = F_{\text{exact}}(t) + \left\{ \frac{2\alpha}{t^4} + \frac{\beta}{t^3} + \frac{\gamma}{t^2} - \left[\frac{2\alpha}{t^4} + \frac{\beta + 2\alpha(\lambda - 1)}{t^3} + \frac{\gamma + \beta(\lambda - 1) + \alpha(\lambda - 1)^2}{t^2} \right] e^{-(\lambda - 1)t} \right\} \eta + \mathcal{O}(\eta^2), \quad (\text{A7})$$

where the low-density behavior of $F_{\text{exact}}(t)$ is given by Eqs. (2.11)–(2.13) and we have called

$$\alpha \equiv -3x(1+x)(\lambda^2 - 1), \quad (\text{A8})$$

$$\beta \equiv \bar{A}_1^{(0)} + 2x(1+x)(\lambda - 1)^2(1 + 2\lambda), \quad (\text{A9})$$

$$\gamma \equiv -\bar{A}_1^{(0)}(\lambda - 1) + \frac{L_1^{(2)}}{\lambda - 1} - x\left(\frac{3}{2}\lambda^4 - 4\lambda^3 + 1\right) - 2x^2(\lambda - 1)^2(3\lambda^2 + 4\lambda + 2) - 3x^3(\lambda^2 - 1)^2. \quad (\text{A10})$$

From Eq. (A7) one can get the difference $\Delta y_1(r)$ between the approximate and the exact coefficient $y_1(r)$ in the density expansion (2.2). The result is

$$\Delta y_1(r) \Theta(r - 1) = \frac{\pi}{6(1+x)r^4} [\alpha(r - 1)^2 + \beta(r - 1) + \gamma] \times [\Theta(r - 1) - \Theta(r - \lambda)]. \quad (\text{A11})$$

Thus, the difference vanishes if $r > \lambda$, regardless the values of $\bar{A}_1^{(0)}$ and $L_1^{(2)}$. Now, the continuity condition (3.12) implies that $\Delta y_1(\lambda) = 0$, which yields

$$L_1^{(2)} = x(\lambda - 1) \left[3x^2(\lambda^2 - 1)^2 + x(\lambda - 1)^2(5\lambda^2 + 10\lambda + 3) + \frac{\lambda}{2}(\lambda^3 - 12\lambda + 8) \right]. \quad (\text{A12})$$

With this value inserted into Eq. (A10), Eq. (A11) becomes Eq. (3.19).

APPENDIX B: THE STICKY-HARD-SPHERE LIMIT

In the limit $x \rightarrow \infty$, $\lambda \rightarrow 1$, $x(\lambda - 1) = 1/12\tau$, Eq. (3.3) reduces to Eq. (3.7) and Eqs. (3.8)–(3.11) become

$$L^{(1)} = (1 + 2\eta)^{-1} (1 + \frac{1}{2}\eta + 6\eta L^{(2)}), \quad (\text{B1})$$

$$S^{(1)} = \frac{\eta}{1 + 2\eta} \left(-\frac{3}{2} + 6L^{(2)} \right), \quad (\text{B2})$$

$$S^{(2)} = \frac{1}{2(1 + 2\eta)} [-1 + \eta + 2(1 - 4\eta)L^{(2)}], \quad (\text{B3})$$

$$S^{(3)} = -\frac{1}{1 + 2\eta} \left[\frac{(1 - \eta)^2}{12\eta} + (1 - \eta)L^{(2)} \right]. \quad (\text{B4})$$

In the SHS limit, Eq. (3.14) is equivalent to

$$(1 + x)\bar{\xi}(0) = x[\xi(0) + \xi'(0)(\lambda - 1)], \quad (\text{B5})$$

where $\xi'(r) \equiv d\xi(r)/dr$. The expression for $\bar{\xi}(0)$ is given by Eq. (3.17) and a similar expression holds for $\xi(0)$. As for $\xi'(0)$, one has

$$\begin{aligned} \xi'(0) &= \lim_{t \rightarrow \infty} t [t^2 R(t) - \xi(0)] \\ &= -\frac{1}{12\eta} \frac{1}{S^{(3)}} \left(A^{(0)} - A^{(1)} \frac{S^{(2)}}{S^{(3)}} \right). \end{aligned} \quad (\text{B6})$$

Making use of Eqs. (3.4)–(3.6) and after taking the SHS limit, Eq. (B5) yields

$$\frac{L^{(1)}}{L^{(2)}} - \frac{S^{(2)}}{S^{(3)}} = 12\tau. \quad (\text{B7})$$

Equations (B1)–(B4) and (B7) constitute the set of algebraic equations satisfied by the parameters of our model in the special case of the SHS fluid. These equations were first derived in Ref. 16 working directly with the SHS fluid. It was shown there that the results coincided with Baxter's solution of the PY equation.¹

When taking the SHS limit, one must distinguish

$$\mathcal{Y}' \equiv \lim_{\lambda \rightarrow 1} y'(\lambda^+) \quad (\text{B8})$$

from

$$\bar{\mathcal{Y}}' \equiv \lim_{\lambda \rightarrow 1} y'(1^+). \quad (\text{B9})$$

The first quantity is

$$\begin{aligned} \mathcal{Y}' &= \lim_{\lambda \rightarrow 1} \left\{ \lambda^{-1} [\xi'(0) + (\lambda - 1)\xi''(0) - \bar{\xi}'(0)] \right. \\ &\quad \left. - \lambda^{-2} [\xi(0) + (\lambda - 1)\xi'(0) - \bar{\xi}(0)] \right\} \\ &= -\frac{1}{12\eta} \frac{1}{S^{(3)}} \left[1 - L^{(2)} \frac{S^{(1)}}{S^{(3)}} + \left(1 + \frac{S^{(2)}}{S^{(3)}} \right) \right. \\ &\quad \left. \times \left(L^{(2)} \frac{S^{(2)}}{S^{(3)}} - L^{(1)} \right) \right], \end{aligned} \quad (\text{B10})$$

where we have taken into account that

$$\xi''(0) = -\frac{1}{12\eta} \frac{1}{S^{(3)}} \left[\left(A^{(1)} \frac{S^{(2)}}{S^{(3)}} - A^{(0)} \right) \frac{S^{(2)}}{S^{(3)}} - A^{(1)} \frac{S^{(1)}}{S^{(3)}} \right]. \quad (\text{B11})$$

The result (B10) was already obtained in Ref. 16. Regarding the quantity $\bar{\mathcal{Y}}'$, our model yields

$$\begin{aligned} \bar{\mathcal{Y}}' &= \lim_{\lambda \rightarrow 1} \frac{1}{1+x} [\xi'(0) - \xi(0)] \\ &= -\frac{1}{12\eta} \frac{1}{S^{(3)}} \left[1 + \left(1 + \frac{S^{(2)}}{S^{(3)}} \right) \left(L^{(2)} \frac{S^{(2)}}{S^{(3)}} - L^{(1)} \right) \right] \\ &= \mathcal{Y}' - \frac{1}{12\eta} \frac{L^{(2)} S^{(1)}}{S^{(3)^2}}. \end{aligned} \quad (\text{B12})$$

In the case of the PY equation, however, one gets¹⁶

$$\bar{\mathcal{Y}}' = \mathcal{Y}' + \frac{1}{24\eta} \left(\frac{L^{(2)}}{S^{(3)}} \right)^3. \quad (\text{B13})$$

APPENDIX C: ONE-DIMENSIONAL SQUARE-WELL FLUIDS

In the one-dimensional case, we introduce the Laplace transform $G(t)$ of $g(r)$:

$$G(t) = \int_1^{\infty} dr e^{-rt} g(r). \quad (C1)$$

Thus, the structure factor is given by

$$S(q) = 1 + 2\eta \operatorname{Re} \lim_{t \rightarrow iq} [G(t) - t^{-1}], \quad (C2)$$

where $\eta \equiv \rho^*$. The auxiliary function $F(t)$ is now defined through the relation¹⁶

$$G(t) = \frac{F(t)e^{-t}}{1 - \eta F(t)e^{-t}} = \sum_{n=1}^{\infty} \eta^{n-1} [F(t)]^n e^{-nt}. \quad (C3)$$

Laplace inversion yields

$$g(r) = \sum_{n=1}^{\infty} \eta^{n-1} f_n(r-n) \Theta(r-n), \quad (C4)$$

where now $f_n(r)$ is the inverse Laplace transform of $[F(t)]^n$. Consequently,

$$g(1^+) = f_1(0) = \lim_{t \rightarrow \infty} t F(t). \quad (C5)$$

In addition, from Eq. (C2) one gets

$$G(t) = t^{-1} + \frac{S(0) - 1}{2\eta} + o(t). \quad (C6)$$

Since $g(1^+)$ must be finite, we conclude that

$$F(t) \sim t^{-1}, \quad t \rightarrow \infty. \quad (C7)$$

On the other hand, since $S(0)$ must also be finite, the first two coefficients in the expansion of $F(t)$ in powers of t are known:

$$F(t) = \frac{1}{\eta} \left[1 + \left(1 - \frac{1}{\eta} \right) t \right] + \mathcal{O}(t^2). \quad (C8)$$

Equations (C1)–(C8) are the one-dimensional counterpart of Eqs. (2.3)–(2.10), respectively, and are exact. As done in Sec. III, our model consists of assuming rational-function forms for the functions $R(t)$ and $\bar{R}(t)$ defined in Eq. (2.11). The functions compatible with (C7) and (C8) containing the least number of parameters are

$$R(t) = \frac{1}{\eta} \frac{A^{(0)}}{1 + S^{(1)}t}, \quad (C9)$$

$$\bar{R}(t) = \frac{1}{\eta} \frac{\bar{A}^{(0)}}{1 + S^{(1)}t}, \quad (C10)$$

where $A^{(0)} = 1 + \bar{A}^{(0)}$ and

$$S^{(1)} = \frac{1}{\eta} - 1 + \bar{A}^{(0)}(\lambda - 1). \quad (C11)$$

To determine $\bar{A}^{(0)}$ we make use of the continuity condition (3.12) or, equivalently, (3.14), where now $\xi(r)$ and $\bar{\xi}(r)$ are the inverse Laplace transforms of $R(t)$ and $\bar{R}(t)$, respectively. The resulting condition is

$$\bar{A}^{(0)} = \left(\frac{1+x}{x} e^{(\lambda-1)/S^{(1)}} - 1 \right)^{-1}. \quad (C12)$$

The solution of this transcendental equation, along with Eq. (C11) allows one to get the parameters needed in the model, Eqs. (C9) and (C10).

In 1953, Salsburg, Zwanzig, and Kirkwood¹⁹ succeeded in deriving the exact distribution function of any one-dimensional fluid whose particles interact via a nearest-neighbor pair potential. This includes the SW interaction with $\lambda < 2$ as a particular case. In this exact solution, the Laplace transform $G(t)$ is given by Eq. (C3) with

$$F(t) = \frac{e^t \Omega(t+c)}{\eta \Omega(c)}, \quad (C13)$$

where

$$\Omega(t) \equiv \int_0^{\infty} dr e^{-rt} e^{-\varphi(r)/k_B T}, \quad (C14)$$

and c is a real constant determined by the condition

$$\frac{1}{\eta} + \frac{\Omega'(c)}{\Omega(c)} = 0. \quad (C15)$$

In the SW case, the function $\Omega(t)$ becomes

$$\Omega(t) = \frac{e^{-t}}{t} (1+x - x e^{-(\lambda-1)t}), \quad (C16)$$

so that Eq. (C13) reduces to

$$F(t) = \frac{1}{\eta} \frac{c}{t+c} \frac{1+x - x e^{-(\lambda-1)(t+c)}}{1+x - x e^{-(\lambda-1)c}} \quad (C17)$$

and c is the solution of the transcendental equation

$$\frac{1}{\eta} = \frac{1}{c} + \frac{1+x - \lambda x e^{-(\lambda-1)c}}{1+x - x e^{-(\lambda-1)c}}. \quad (C18)$$

Now, if we identify $S^{(1)} = 1/c$, $\bar{A}^{(0)} = [e^{(\lambda-1)c}(1+x)/x - 1]^{-1}$, the exact expression (C17) coincides with that of our model, Eqs. (2.11), (C9), and (C10). Equation (C18) is then equivalent to Eq. (C11).

¹R. J. Baxter, *J. Chem. Phys.* **49**, 2770 (1968).

²J. A. Barker and D. Henderson, *Rev. Mod. Phys.* **48**, 587 (1976).

³J. A. Barker and D. Henderson, *Mol. Phys.* **21**, 187 (1971).

⁴D. Henderson, W. G. Madden, and D. D. Fitts, *J. Chem. Phys.* **64**, 5062 (1976).

⁵D. Henderson, O. H. Scalise, and W. R. Smith, *J. Chem. Phys.* **72**, 2431 (1980).

⁶D. Henderson (private communication).

⁷J. S. Huang, S. A. Safran, M. W. Kim, G. S. Grest, M. Kotlarchyk, and N. Quirke, *Phys. Rev. Lett.* **53**, 592 (1984).

⁸P. V. Sharma and K. C. Sharma, *Physica A* **89**, 203 (1977).

⁹M. S. Wertheim, *Phys. Rev. Lett.* **10**, 321 (1963); E. Thiele, *J. Chem. Phys.* **39**, 474 (1963).

¹⁰N. A. Seaton and E. D. Glandt, *J. Chem. Phys.* **86**, 4668 (1987).

¹¹S. V. G. Menon, C. Manohar, and K. Srinivasa Rao, *J. Chem. Phys.* **95**, 9186 (1991).

- ¹²C. Regnaut and J. C. Ravey, *J. Chem. Phys.* **91**, 1211 (1989); **92**, 3250 (1990).
- ¹³C. Robertus, J. G. H. Joosten, and Y. K. Levine, *Phys. Rev. A* **42**, 4820 (1990).
- ¹⁴C. G. de Kruif, P. W. Rouw, W. J. Briels, M. H. G. Duits, A. Vrij, and R. P. May, *Langmuir* **5**, 422 (1989); M. H. G. Duits, R. P. May, A. Vrij, and C. G. de Kruif, *Langmuir* **7**, 62 (1991).
- ¹⁵S. Bravo Yuste and A. Santos, *Phys. Rev. A* **43**, 5418 (1991).
- ¹⁶S. Bravo Yuste and A. Santos, *J. Stat. Phys.* **72**, 703 (1993).
- ¹⁷S. Bravo Yuste and A. Santos, *Phys. Rev. E* **48**, 4599 (1993).
- ¹⁸J. A. Barker and D. Henderson, *Can. J. Phys.* **45**, 3959 (1967). Note a misprint in the fourth line of Eq. (19): the term $\lambda^3 r$ should read $\lambda^2 r$.
- ¹⁹Z. W. Salsburg, R. W. Zwanzig, and J. G. Kirkwood, *J. Chem. Phys.* **21**, 1098 (1953).
- ²⁰The simulation values of $g(1^+)$ at $\lambda = 1$ have been obtained from those of a HS fluid, $g_{\text{HS}}(1^+)$, by following the chain of equations $\lim_{\lambda \rightarrow 1} g(1^+) = \lim_{\lambda \rightarrow 1} g(\lambda^-) = (1+x) \lim_{\lambda \rightarrow 1} g(\lambda^+) = (1+x) g_{\text{HS}}(1^+)$.
- ²¹S. C. Netemeyer and E. D. Glandt, *J. Chem. Phys.* **85**, 6054 (1986).
- ²²Y. C. Chiew and E. D. Glandt, *J. Phys. A* **16**, 2599 (1983); W. G. T. Kranendonk and D. Frenkel, *Mol. Phys.* **64**, 403 (1988); G. Stell, *J. Stat. Phys.* **63**, 1203 (1991); S. B. Lee, *J. Chem. Phys.* **98**, 8119 (1993).
- ²³As a matter of fact, we have used a computer algebra system. See S. Wolfram, *Mathematica: A System for Doing Mathematics by Computer* (Addison-Wesley, Redwood City, 1991).